



The microbiota-dependent tryptophan metabolite alleviates high-fat diet-induced insulin resistance through the hepatic AhR/TSC2/mTORC1 axis

Wei Du^{a,1} , Shanshan Jiang^{b,1}, Shengxiang Yin^b, Rongjiang Wang^b, Chunling Zhang^b, Bin-Cheng Yin^a, Jialin Li^c, Li Li^c, Nan Qi^{b,d,2}, Ying Zhou^{a,2} and Bang-Ce Yea,b,2

Affiliations are included on p. 11.

Edited by Dennis Kasper, Harvard Medical School, Boston, MA; received January 8, 2024; accepted July 23, 2024

Type 2 diabetes (T2D) is potentially linked to disordered tryptophan metabolism that attributes to the intricate interplay among diet, gut microbiota, and host physiology. However, underlying mechanisms are substantially unknown. Comparing the gut microbiome and metabolome differences in mice fed a normal diet (ND) and high-fat diet (HFD), we uncover that the gut microbiota-dependent tryptophan metabolite 5-hydroxyindole-3-acetic acid (5-HIAA) is present at lower concentrations in mice with versus without insulin resistance. We further demonstrate that the microbial transformation of tryptophan into 5-HIAA is mediated by Burkholderia spp. Additionally, we show that the administration of 5-HIAA improves glucose intolerance and obesity in HFD-fed mice, while preserving hepatic insulin sensitivity. Mechanistically, 5-HIAA promotes hepatic insulin signaling by directly activating AhR, which stimulates TSC2 transcription and thus inhibits mTORC1 signaling. Moreover, T2D patients exhibit decreased fecal levels of 5-HIAA. Our findings identify a noncanonical pathway of microbially producing 5-HIAA from tryptophan and indicate that 5-HIAA might alleviate the pathogenesis of T2D.

gut microbiota | tryptophan metabolism | insulin signaling | type 2 diabetes

Type 2 diabetes (T2D) is a widespread, metabolic disorder caused by multiple genetic and environmental factors. Increasing evidence supports the key role of gut microbiotahost interactions in the pathogenesis of diet-induced T2D (1-3). Particularly, the dietary overindulgence such as a high-fat diet (HFD) leads to changes in the gut microbial composition, termed dysbiosis, which disrupts the homeostasis of the gut-liver axis and impairs the metabolic function of the liver via microbially produced or dependent metabolites [e.g., short-chain fatty acids (SCFAs), secondary bile acids, and trimethylamine-N-oxide (TMAO)] (4). Hepatic insulin resistance (IR) and impaired insulin signaling, as a result of progressive liver dysfunction, contribute to the abnormal glucose metabolism and glucose intolerance in T2D patients (5). Therefore, studying the microbiome and metabolome between gut-liver cross talk is crucial for screening potential pharmaceutical agents to improve IR and treat T2D.

It has emerged that aromatic amino acids (AAAs) tryptophan (Trp), phenylalanine, and tyrosine, as well as their bioactive metabolites produced via the gut microbial pathway, are potentially correlated with T2D pathogenesis (6–8). As the largest AAA by molecular weight, Trp is taken up and catabolized in the gastrointestinal tract where the commensal bacteria degrade it. Three major pathways account for intestinal Trp metabolism and its role in the host–microbiota cross talk (9). i) The indole/aryl hydrocarbon receptor (AhR) pathway. Numerous bacterial species (e.g., Escherichia coli, Clostridium spp., and Bacteroides spp.) can directly convert Trp into indole and its derivatives such as indole-3-acetic acid (ÎAA), which activate the AhR signaling and subsequently regulate intestinal homeostasis (4). ii) The Kynurenine (Kyn) pathway. Intestinal Trp can be transformed into Kyn by indoleamine 2,3-dioxygenase (IDO) 1 under bacterial regulation in immune and epithelial cells (10). iii) The serotonin [5-hydroxytryptamine (5-HT)] pathway. Above 90% of the neurotransmitter 5-HT is produced in enterochromaffin cells (ECs) in the gut, where Trp is catalyzed into 5-hydroxytryptophan (5-HTP) by Trp hydroxylase 1 enzyme (TPH1) and is further transformed into 5-HT by aromatic amino acid decarboxylase (AAAD). Gut microbial metabolites such as SCFAs and deoxycholate can stimulate TPH1 expression, thereby enhancing the biosynthesis of 5-HT (11, 12).

Recent studies suggest a central role of impaired Trp metabolism through the 5-HT pathway in gut microbiota-host cross talk regarding metabolic syndromes such as obesity and diabetes. Gut-derived 5-HT produced under the control of microbiota is positively

Significance

High-fat diet (HFD) causes the dysbiosis of the gut microbiota, which influences the host glucose metabolism and thus leads to type 2 diabetes (T2D). Determination of the microbial metabolism pathway and certain agents contributing to T2D are pivotal for the therapeutic strategies. Here, we report that the HFD-induced gut microbiota dysbiosis of mice results in a depletion of 5-HIAA from disordered tryptophan metabolism involving the gut bacteria Burkholderia spp. and specific microbial enzymes. The results emphasize the value of 5-HIAA as a potential therapeutic agent since 5-HIAA can improve the glucose intolerance in vivo by promoting hepatic insulin signaling. More importantly, the decreased fecal levels of 5-HIAA might be considered as a premonitory diagnostic sign of T2D.

Author contributions: B.-C. Ye designed research; W.D., S.-S.J., S.-X.Y., R.-J.W., and C.-L.Z. performed research; W.D., S.-S.J., S-X.Y., C.-L.Z., J.-L.L., L.L., N.Q., and Y.Z. contributed new reagents/analytic tools; W.D., B.-C. Yin, N.Q., Y.Z., and B.-C. Ye analyzed data; and W.D., N.Q., Y.Z., and B.-C. Ye wrote the paper.

The authors declare no competing interest.

This article is a PNAS Direct Submission.

Copyright © 2024 the Author(s). Published by PNAS. This article is distributed under Creative Commons Attribution-NonCommercial-NoDerivatives License 4.0 (CC BY-NC-ND).

¹W.D. and S.-S.J. contributed equally to this work.

²To whom correspondence may be addressed. Email: qi_nan@gzlab.ac.cn, zhouying@ecust.edu.cn, or bcye@

This article contains supporting information online at https://www.pnas.org/lookup/suppl/doi:10.1073/pnas. 2400385121/-/DCSupplemental.

Published August 21, 2024.

correlated with metabolic syndrome, as circulating 5-HT levels were reported to be elevated in obese subjects (13). Although brain-derived 5-HT induces satiety, gut-derived 5-HT stimulates fasting-induced lipolysis in adipose tissues, promotes liver gluconeogenesis, and prevents glucose uptake by hepatocytes, thus favoring maintenance of blood glucose levels (14). Furthermore, chemical inhibition or genetic deletion of gut-derived 5-HT biosynthesis, as well as antibiotic-induced changes in gut microbiota composition, have been shown to protect HFD-fed mice against obesity and glucose intolerance (15). In spite of that, the specific role of the microbiota in intestinal Trp metabolism is still opaque. It is also unknown whether there are other microbiota-dependent Trp metabolites regulating glucose homeostasis in response to a given diet. AhR, a ligand-dependent transcription factor with multiple effects, is expressed in a wide range of cell types including intestine cells, immune cells, and hepatic cells. It is well known for the regulatory role of AhR in intestinal mucosal homeostasis and immune cell development and function (16, 17). However, whether the hepatic AhR signaling is involved in the maintenance of glucose homeostasis remains to be elucidated.

Herein, we perform differential analysis of the gut microbiome and metabolome between mice fed a HFD and normal diet (ND). We show that 5-hydroxyindole-3-acetic acid (5-HIAA), a Trp metabolite downstream of 5-HT, is depleted in the serum and feces of HFD-fed mice with IR. We further unveil the microbial production of 5-HIAA from Trp in vitro and characterize the bioactivity of 5-HIAA in improving glucose intolerance in vivo. Moreover, we dissect the underlying mechanism by which 5-HIAA promotes hepatic insulin signaling and protects insulin sensitivity. Finally, we compare the 5-HIAA levels of clinical samples from subjects with and without T2D. Our study unveils a regulatory role of the gut microbiota—dependent 5-HIAA in T2D pathogenesis and provides insights into the utilization of 5-HIAA as a potential therapeutic agent for T2D.

Results

HFD-Induced IR Mice Undergo Alterations in the Gut Microbiome.

To study the diet-gut microbiota-host interactions involving T2D pathogenesis, we first established an IR mice model by HFD feeding. Male C57BL/6J mice at the age of 4 wk were maintained on ND or HFD for 15 wk, respectively, with fasting body weights, plasma levels of glucose, and insulin to be weekly measured. During the course of feeding, HFD mice progressively gained more weight than ND mice and developed fasting hyperglycemia (Fig. 1 *A* and *B*). After a 6-wk feeding, impaired glucose tolerance and insulin tolerance can be observed in HFD mice (SI Appendix, Fig. S1 A and B). At the end point, HFD mice exhibited IR as revealed by the Homeostasis Model Assessment (HOMA) index (Fig. 1*C*). Furthermore, administration of HFD significantly reduced the protein levels of insulin receptor substrate 1 and 2 (IRS1 and IRS2) in the liver, indicating a compromised hepatic insulin signaling in HFD mice (Fig. 1D). All these results suggest a progressive worsening of IR in mice during HFD feeding.

Next, we sought to characterize the features of the gut microbiome in HFD-induced IR mice. For this purpose, we collected the feces of ND mice and HFD mice at the end point and conducted integrated 16S rDNA sequencing and metagenomic differential analysis (*SI Appendix*, Fig. S1C). After quality control and similarity cluster analysis of the 16S rDNA sequencing data, 76,071 ± 2,877 clean reads per sample and 2,804 OTUs were obtained. As a comprehensive indicator reflecting the species richness and uniformity, the alpha diversity of each sample was calculated to measure the species richness in the microbial

community ecology. No obvious difference was found in the curves of four alpha diversity indexes between the ND group and the HFD group, suggesting that HFD feeding did not influence the evenness and stability of the gut microbial community in mice (SI Appendix, Fig. S2A). Indeed, HFD feeding significantly altered the gut microbiota composition in mice, as revealed by the two-dimensional principal component analysis (PCA) score plot (Fig. 1E).

Furthermore, we dissected the HFD-induced alterations of gut microbiota composition. Differences between the relative abundance of gut bacteria in ND mice and HFD mice were analyzed by the t test and Mann–Whitney U test. When compared to ND mice, HFD mice showed a decrease in the relative abundance of Bacteroidetes (73.39% vs. 83.73%, P < 0.001, q < 0.05) and a higher portion of *Firmicutes* (24.11% vs. 13.7%, P < 0.001, q < 0.05) in the gut microbial community (Fig. 1*F*). The gut microbiomic profile of HFD mice at the phylum level was consistent with that of obese people (18). It was noticed that the bacteria with significant alterations in the relative abundance belong to the genus Muribaculum, Bacteroides, Lachnospiraceae, Parabacteroides, Muribaculaceae_unclassified, Prevotellaceae_UCG-001, and Lachnospiraceae_NK4A136_group (Fig. 1G). At the species level, the relative abundance of s_ Muribaculaceae, s_Prevotellaceae_UCG-001, s_Lactobacillus_ $iatae, s_Muribaculum_sp, s_Lachnospiraceae, s_Anaerotignum_sp.,$ s_Lachnospiraceae_NK4A136_group, s_Bacteroides_acidifaciens, and s_Parabacteroides_unclassified was substantially changed in the colon of HFD mice (SI Appendix, Fig. S2B). These data above display the HFD-induced alterations in the gut microbiome of IR mice.

5-HIAA Is Depleted in HFD-Induced IR Mice. To determine the alterations in the gut metabolome of HFD-induced IR mice, we performed the metabolomic profiling of the above mice fecal samples by HPLC-ESI-QTOF-MS analysis. The partial least squares-discriminate analysis (PLS-DA) plot of differential metabolites showed significant variations between the gut metabolome of mice fed a ND and HFD (Fig. 2 A and B). According to the above manipulations, potential variables were chosen as biomarkers based on VIP > 1, P < 0.05, and fold change > 2. There were 7,813 features detected, with 756 up-regulated and 336 down-regulated (Fig. 2C). We further annotated the differentially produced metabolites in the Kyoto Encyclopedia of Genes and Genomes (KEGG) pathway, revealing that HFD predominantly impaired 20 metabolic pathways including the biosynthesis of unsaturated fatty acids, phenylalanine metabolism, tyrosine metabolism, and Trp metabolism (Fig. 2D).

Previous studies suggested a potential role of Trp metabolism in the gut microbiota-host cross talk in T2D and other metabolic syndromes, while leaving the underlying mechanisms to be further investigated (14, 19). Consistently, an impaired Trp metabolism has been found in the gut of HFD-induced IR mice herein, inspiring us to identify the functional Trp metabolites contributing to T2D pathogenesis. We thus conducted differential analysis of metabolites in the Trp metabolic pathway based on the untargeted fecal metabolomic profiles of ND mice and HFD mice (SI Appendix, Fig. S3). It was noticed that 5-HIAA, a Trp metabolite downstream of 5-HT, was present at lower levels in the feces of HFD mice than ND mice (Fig. 2*E*). To confirm this finding, we developed a targeted HPLC-MS/MS method for measuring the fecal and serum levels of 5-HIAA in mice fed a HFD and ND (SI Appendix, Fig. S4). As expected, 5-HIAA was decreased in the feces and sera of HFD mice when compared to those of ND mice (Fig. 2F). We thus conclude

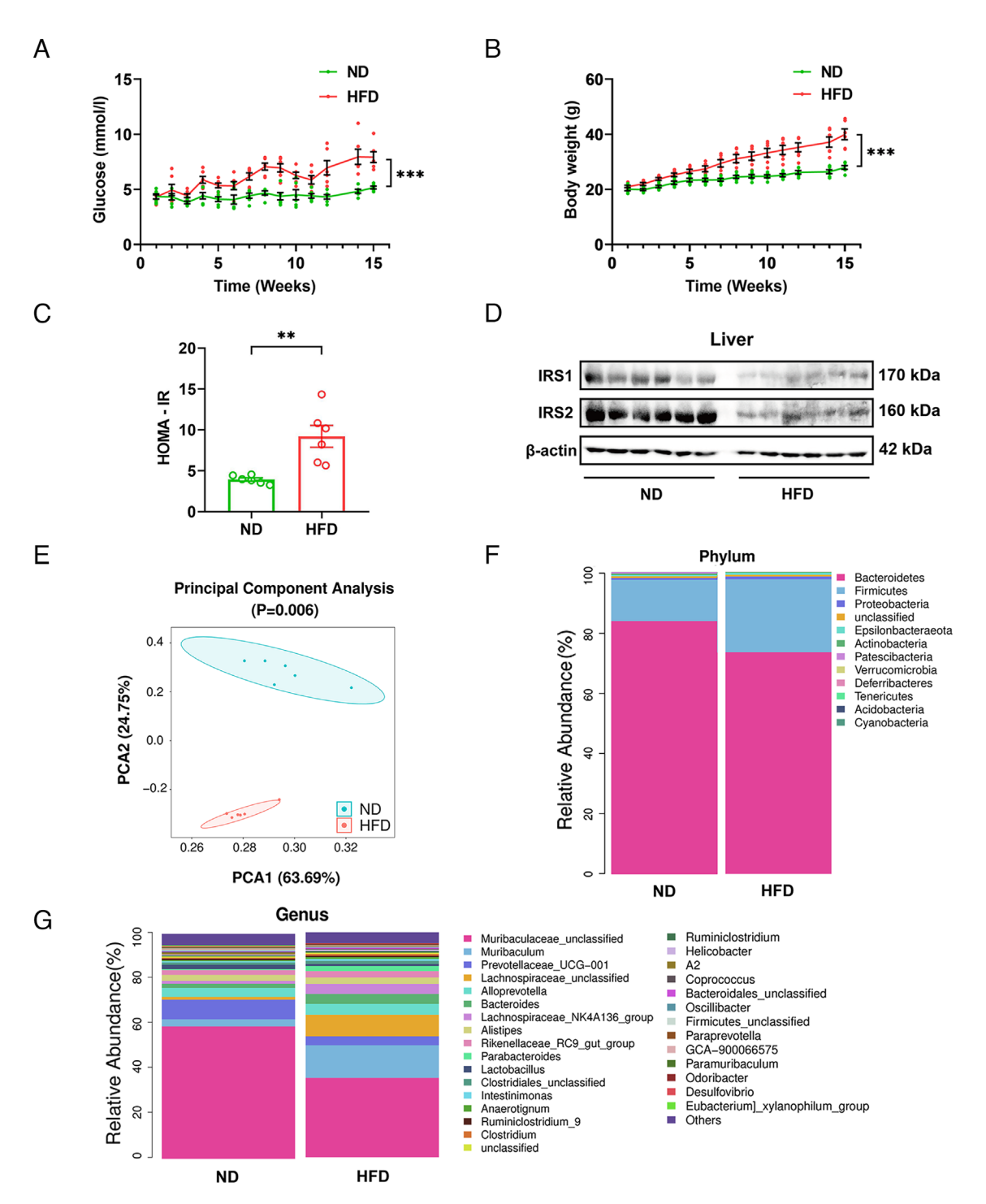


Fig. 1. HFD feeding induces IR and causes alterations of the gut microbiome in mice. Male C57BL/6J mice (4 wk old) were fed a HFD (n = 6) or ND (n = 6) for 15 wk. See also SI Appendix, Fig. S1C. (A) Blood glucose curves. (B) Body weight curves. (C) Homeostasis Model Assessment of IR (HOMA-IR) at the end point. (D) Immunoblotting analysis of IRS1 and IRS2 protein levels in liver tissues. (E) Two-dimensional principal coordinates analysis (PCA) plot of the gut microbiota composition. Scores are based on the relative abundance of operational taxonomic units (OTUs). Each symbol represents an individual mouse. See also SI Appendix, Fig. S2A. (F) Barplot analysis of the phylum level of the gut microbial community. (G) Barplot analysis of the genus level of the gut microbial community. Data are shown as mean \pm SEM. (A-C; n = G) or are representative of three independent experiments with similar results (D). *P < 0.05, **P < 0.01, and ***P < 0.005. Statistical analysis was performed using unpaired two-tailed Student's t test (A-C).

that 5-HIAA is diminished through the impaired Trp metabolism in HFD-induced IR mice.

5-HIAA Can be Microbially Produced from Trp through a **Noncanonical Pathway In Vivo.** As illustrated in Fig. 3A, it is traditionally believed that the transformation of intestinal Trp into 5-HIAA through canonical 5-HT pathway is host cell dependent and undergoes the microbial regulation (11, 12). Since the genes

encoding key enzymes for 5-HIAA production such as monoamine oxidase (MAO) are also found in the microbial genome, we addressed whether 5-HIAA can be host-independently produced from Trp by the gut microbiota. We challenged the microbial communities in fecal suspensions from mice with Trp, 5-HTP, and 5-HT for 24 h, respectively, and then measured the concentrations of 5-HIAA. To demonstrate the microbial contribution, a control group was set by pretreating the fecal microbiota with a cocktail of

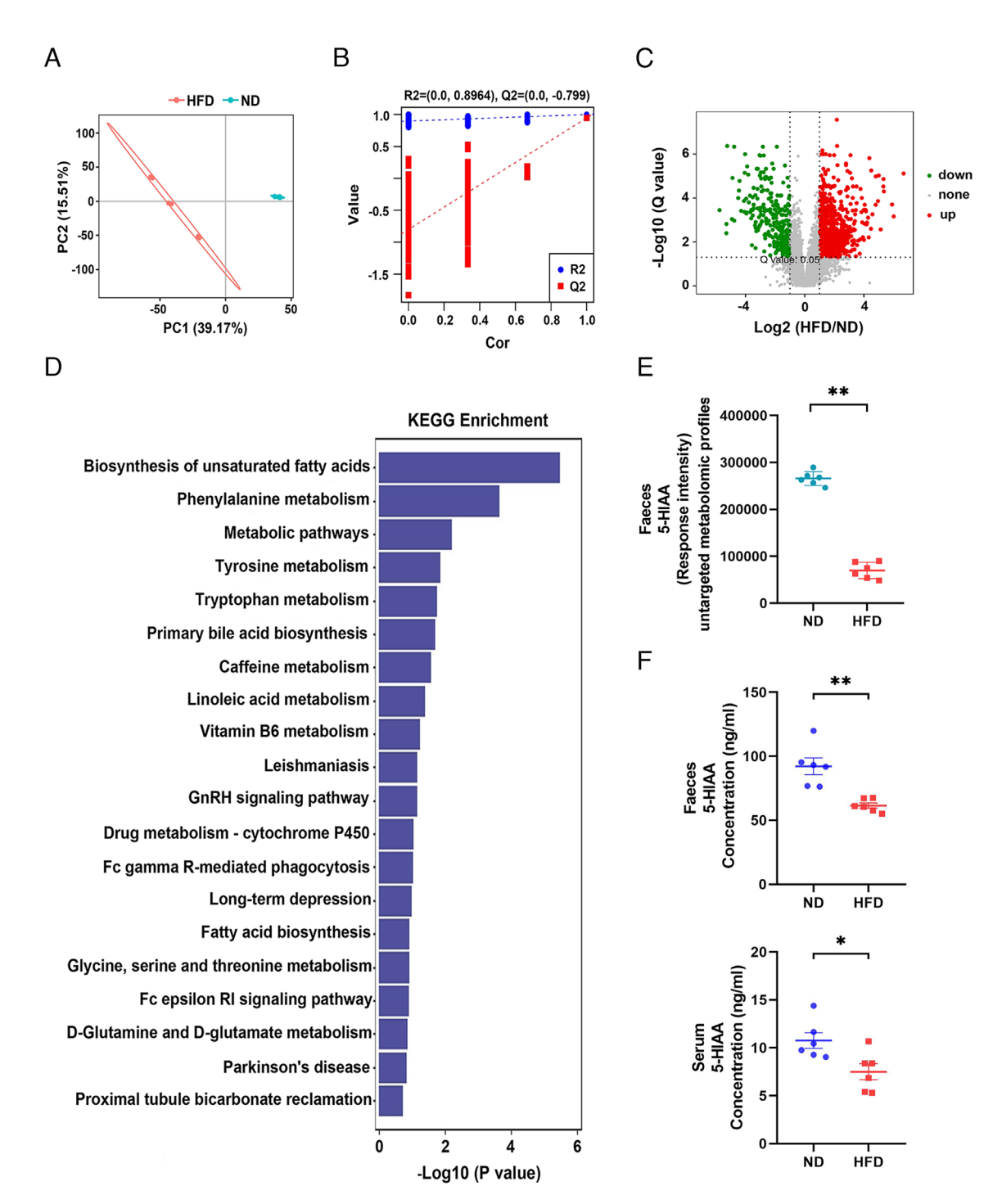


Fig. 2. HFD-fed mice exhibit altered gut metabolome and decreased 5-HIAA concentrations. Metabolomic analysis of samples collected from HFD mice and ND mice (*n* = 6 per group) as in Fig. 1. See also *SI Appendix*, Fig. S1. (*A*) The PLS-DA plot of differential metabolites from fecal samples. Each symbol represents an individual mouse. (*B*) Permutation test of CK-P1 showing the robustness of the PLS-DA model. (*C*) Volcano plots of differential metabolites that were up-regulated (red) or down-regulated (green) in fecal samples (HFD group vs. ND group). The broken line denotes a cutoff q value < 0.05 (Student's *t* test). (*D*) Overview of enriched KEGG pathways of metabolites. (*E*) Untargeted metabolomic profiling was performed using the same fecal samples of HFD mice and ND mice as in Fig. 1. The intensity of 5-HIAA in the feces of HFD mice and ND mice. (*F*) Targeted HPLC-MS/MS analysis determining the fecal and serum levels of 5-HIAA. Each symbol represents an individual mouse. See also *SI Appendix*, Figs. S3 and S4. Data are shown as mean ± SEM. (*n* = 6). **P* < 0.05 and ***P* < 0.01. Statistical analysis was performed using unpaired two-tailed Student's *t* test (*E* and *F*).

broad-spectrum antibiotics (Abx). We detected marked 5-HIAA production during microbial catalysis of Trp and 5-HTP, but failed to observe statistical difference in the basal 5-HIAA levels between batch culture of fecal microbiota with and without 5-HT (Fig. 3B). This basal 5-HIAA is probably generated by the microbial catalysis of native Trp in culture media. We further sought to detect other metabolites in the canonical 5-HT pathway during microbial Trp catalysis and found that 5-HTP but not

5-HT can be produced (*SI Appendix*, Fig. S7A). These results provide evidence that 5-HIAA can be microbially produced from Trp, and indicate that this microbial metabolic pathway that is independent of the canonical 5-HT pathway.

To clarify the conversion of Trp to 5-HTP by gut microbiota, we conducted an in-depth homology analysis on luz15 enzymes, which display Trp-to-5-HTP conversion activity, derived from the *Streptomyces albus* J1074 strain (20). The homologous enzymes of

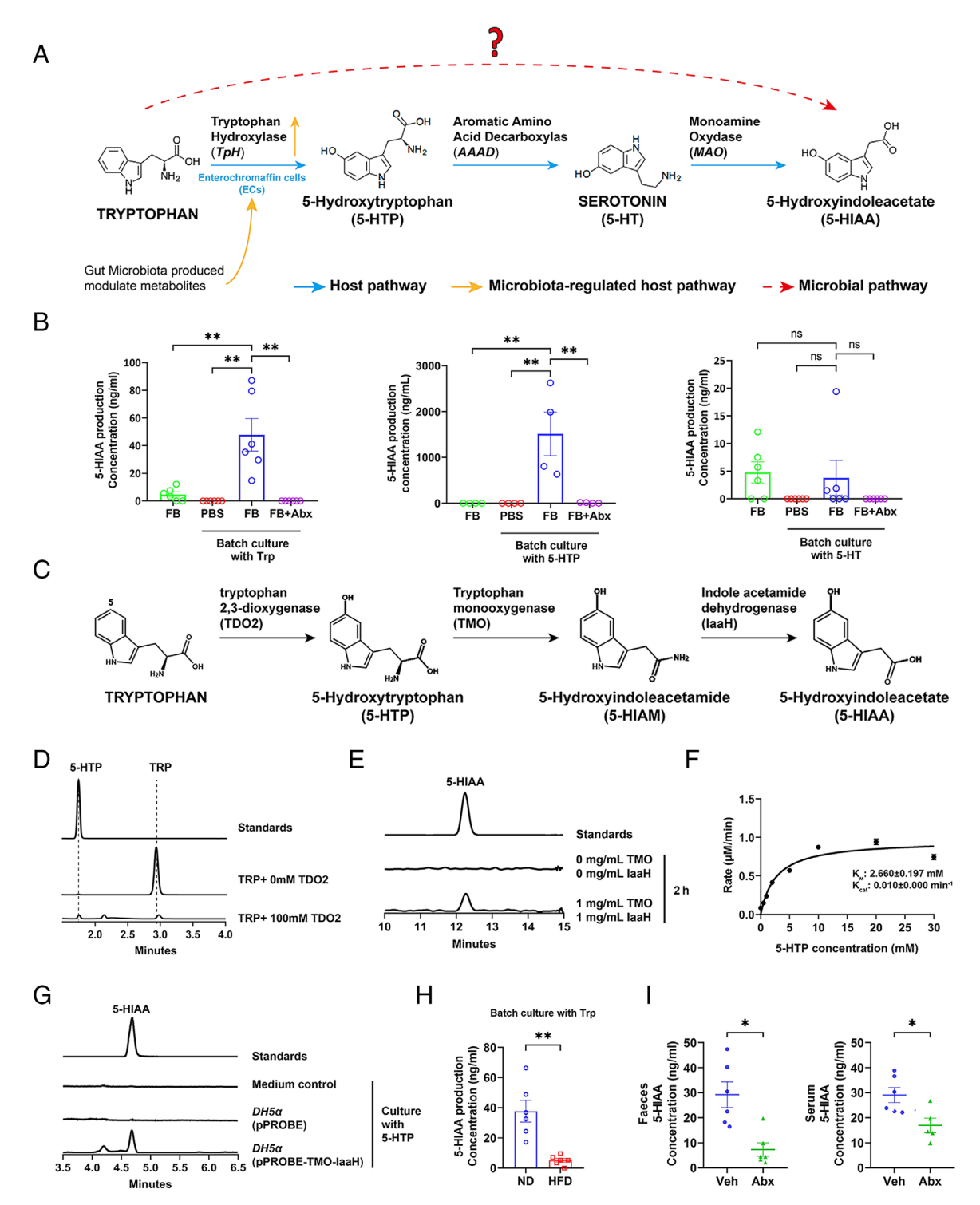


Fig. 3. Burkholderia spp. are responsible for microbially producing 5-HIAA from Trp in the 5-HT-independent pathway. (A) Overview of the metabolic pathway transforming Trp into 5-HIAA. (B) Microbial transformation of Trp, 5-HTP, and 5-HT into 5-HIAA in vitro. Fecal bacteria suspensions (FB) were obtained from 8-wk-old C57BL/6 mice and were then incubated with (blue) or without (green) Trp (10 mM, Left), 5-HTP (10 mM, Middle), or 5HT (10 mM, Right) for 24 h. The concentration of 5-HIAA was measured by LC-MS analysis. PBS (red) and antibiotic cocktails (Abx) treated 6 h (FB+Abx, purple) as negative control. (C) A proposed pathway for transforming Trp into 5-HIAA in the gut. (D) UV-Visible spectra showing the activity of purified TDO2 from Burkholderia cenocepacia in vitro. Purified TDO2 was incubated with Trp (1 mg/mL) for 1 h. (E) Extracted LC-MS/MS ion chromatograms showing the activity of TMO and laaH purified from Burkholderia pyrrocinia in vitro. Purified TMO and laaH were incubated with 5-HTP (1 mg/mL) for 2 h. The reaction mixture was analyzed by LC-MS. (F) Apparent kinetic analysis of TMO-laaH mixed enzyme catalyzes 5-HTP to 5-HIAA. Rate (µM 5-HTP/min) vs. substrate concentration (mM 5-HTP) curve for 5-HTP metabolism by TMO and laaH. Enzymes were incubated with concentrations of 5-HTP that varied from 0.5 to 30 mM. GraphPad was used to fit the Michaelis-Menten curve. See also (SI Appendix, Fig. S7 B–D). (G) Extracted LC–MS/MS ion chromatograms showing the conversion of 5-HTP to 5-HIAA by engineered E. coli. Engineered E. coli DH5α harboring TMO and laaH was grown aerobically in LB Broth containing 5-HTP (1 g/L) at 37 °C for 48 h and analyzed using LC-MS. See also SI Appendix, Fig. S6E. (H) Fecal bacteria suspensions were obtained from ND mice (n = 6 per group) and HFD mice (n = 6 per group) as in Fig. 1 and were then incubated with Trp (10 mM) for 24 h. The concentration of 5-HIAA was measured by LC-MS analysis. (/) Impacts of antibiotic cocktails (Abx) on the production of 5-HIAA in vivo. Male C57BL/6J mice (6 wk old; n = 6 per group) were orally administered with vehicle (Veh) and Abx for 14 d. Fecal and serum levels of 5-HIAA were measured by targeted HPLC-MS/MS. Each symbol represents an individual mouse (B, H, and I). Data are shown as mean ± SEM. (B, H, and I, n = 4 or 6) or mean ± SD. (F, three independent experiments) or are representative of three independent experiments with similar results (D, E, and G). *P < 0.05, **P < 0.01, and ***P < 0.005; ns, not significant. Statistical analysis was performed using the Bonferroni post hoc test followed by one-way ANOVA (B) or unpaired two-tailed Student's t test (H and I).

luz15 were predominantly detected in the phyla Actinomyces, Pseudomonas, and Bacillus (SI Appendix, Fig. S6A). To determine the presence of these enzymes in the gut microbiota, metagenomic analyses were performed on mouse fecal samples. The results revealed the presence of 192 microbial strains in the mouse gut microbiota, possessing enzymes homologous to luz15 (SI Appendix, Fig. S6B). Some of these strains might facilitate the conversion of Trp to 5-HTP. The top 20 strains are enumerated according to their relative abundance (SI Appendix, Fig. S6C). Among these bacterial species, we observed that Burkholderia cenocepacia exhibits the potential to convert Trp into 5-HTP (SI Appendix, Fig. S6D). Subsequently, we purified TDO2 (homologous to Luz15) from B. cenocepacia (SI Appendix, Fig. S6E). Enzymatic experiments demonstrated that B. cenocepacia is capable of converting Trp into 5-HTP through the action of the TDO2 enzyme (Fig. 3D). Through an in-depth investigation of Burkholderia spp., we found that tryptophan monooxygenase (TMO) and Indole acetamide dehydrogenase (IaaH) of Burkholderia pyrrocinia were known to transform Trp into indoleacetic acid (IAA) (21). Trp and 5-HTP as well as IAA and 5-HIAA are structurally similar, with the only difference being a hydroxyl group. These structural similarities may lead to similar metabolic pathways in the organisms. Furthermore, TMO and IaaH enzymes exhibit a high degree of conservation (>90%) between B. cenocepacia and B. pyrrocinia (SI Appendix, Fig. S8). We thus hypothesized that the noncanonical pathway for microbially producing 5-HIAA from 5-HTP is potentially mediated by TMO and IaaH in *B. cenocepacia* and *B.* pyrrocinia (Fig. 3C). To test our hypothesis, we incubated 5-HTP with recombinant TMO and IaaH of B. pyrrocinia. The LC-MS/ MS analysis detected the signal of 5-HIAA in the reaction mixture with TMO and IaaH, indicating that 5-HIAA was generated from 5-HTP under this condition (Fig. 3E). We also estimated the activity of TMO-IaaH-mixed enzyme by time-course analysis and optimizing the TMO/IaaH ratio (SI Appendix, Fig. S7 B-D). Furthermore, we determined the apparent kinetic parameters by showing that the TMO-IaaH-mixed enzyme efficiently catalyzed the oxidization of 5-HTP with k_{cat} , K_M , and k_{cat}/K_M values of 0.01 $\pm 0.00 \text{ min}^{-1}$, 2.660 $\pm 0.197 \text{ mM}$, and 0.0038 min⁻¹/mM⁻¹, respectively (Fig. 3F).

Finally, we generated a *E. coli* DH5α strain expressing FLAG-tagged TMO and IaaH (SI Appendix, Fig. S7E). As expected, this engineered strain was capable of transforming 5-HTP into 5-HIAA (Fig. 3G). Our data thus identify TDO2, TMO, and IaaH as the key enzymes for microbially producing 5-HIAA from Trp in the 5-HT-independent pathway. Next, we compared the capabilities of fecal microbiota in producing 5-HIAA between HFD mice and ND mice. Consistent with the result showing diminished fecal levels of 5-HIAA in HFD mice, the microbial communities from HFD mice fecal suspensions could barely transformed Trp into 5-HIAA when compared to the ND group (Fig. 3H), suggesting that HFD affects the relative abundance of gut bacteria responsible for 5-HIAA production. Furthermore, we generated the Spearman correlation matrix to explore a possible correlation between the gut bacteria and the production of 5-HIAA (SI Appendix, Fig. S5A). It was found that the 5-HIAA production was positively correlated with seven genera (R > 0.8, P < 0.05; Red) and negatively correlated with five genera (R < -0.8, P < 0.05; Blue), respectively (SI Appendix, Fig. S5B). To validate the gut microbial contribution to the production of 5-HIAA, we administered mice orally with Abx for 2 wk, a previously described method for suppressing the gut microbiota (22). As shown in Fig. 31, both fecal and serum levels of 5-HIAA were decreased in mice treated with Abx versus with vehicle. After the Abx treatment, mice were maintained for a 4-wk washout period to permit the repopulation of conventional gut commensals. We detected that the baseline 5-HIAA levels (Pre-Abx) in mice feces dramatically dropped after the 2-wk Abx treatment and then restored following a 4-wk discontinuation of antibiotics (Post-Abx) (*SI Appendix*, Fig. S5C). Altogether, our findings reveal a tight connection among HFD, the gut microbiota, and the microbiota-dependent Trp metabolite 5-HIAA.

5-HIAA Improves Glucose Intolerance and Obesity While **Preserving Hepatic Insulin Sensitivity.** Since a negative correlation has been analytically indicated between the IR of HFD-fed mice and the microbiota-dependent 5-HIAA, we conducted in vivo and in vitro assays to examine whether 5-HIAA has a bioactivity in improving IR. To perform the glucose tolerance test (OGTT) and insulin tolerance test (ITT), mice were fed a ND or HFD for 6 wk, with oral administration of 5-HIAA or vehicle twice a day. After fasting at the end point, mice were orally given glucose or intraperitoneally injected with insulin and then measured the blood glucose levels at different time points. It was suggested that the administration of 5-HIAA improved glucose intolerance and insulin intolerance, as both the acute glycemic response to glucose challenge and insulin-stimulated hypoglycemic level were significantly reduced in HFD mice administered with 5-HIAA verse with vehicle (Fig. 4 A-D). Additionally, we observed a significant reduction in body weight of HFD mice upon administration of 5-HIAA (Fig. 4E). To investigate the distribution of fat mass, we conducted MRI experiment and observed a significant reduction in fat accumulation in HFD mice with 5-HIAA treatment (Fig. 4F). Furthermore, we measured epididymal adipose tissue (eAT), inguinal adipose tissue (iAT), and brown adipose tissue (BAT), and all of them showed significant weight loss (Fig. 4G). The organ weight result also demonstrated that treatment with 5-HIAA could effectively mitigate hepatic and renal hypertrophy in HFD mice (Fig. 4H). To mimic the hepatic IR in vitro, mice primary hepatocytes and human hepatocellular carcinomas HepG2 cells were treated with high concentration insulin (789 mM) and TNF-α (200 ng/mL) for 24 h, respectively, which was previously demonstrated to result in a compromised insulin signaling (23). Incubation of the IR primary hepatocytes with 5-HIAA dose dependently restored the decreased levels of insulin-promoted IRS1 tyrosine phosphorylation and the downstream Akt phosphorylation, suggesting that 5-HIAA can promote hepatic insulin signaling and thus protects insulin sensitivity (Fig. 41). In line with this, 5-HIAA markedly offset the negative effects of TNF- α on hepatic insulin signaling, as the TNF-α-induced alterations of Akt and GSK-3β phosphorylation in HepG2 cells were turned over by 5-HIAA treatment (Fig. 4/). Taken together, these results indicate that the gut microbiotadependent 5-HIAA improves glucose intolerance and hepatic IR by promoting insulin signaling.

5-HIAA Promotes Insulin Signaling Through Activation of the Hepatic AhR/TSC2/mTORC1 Axis. Mammalian target of rapamycin complex 1 (mTORC1), an evolutionary conserved complex containing the protein kinase mTOR, serves as a master regulator for many fundamental cellular processes such as growth, survival, and metabolism. It is known that insulin stimulates cell growth by activation of Akt and mTOR, whereas hyperactivation of the mTORC1 pathway via high concentration insulin and TNF-α impairs insulin signaling by inducing the serine phosphorylation of IRS1 and thus inhibiting its tyrosine phosphorylation (23). Since 5-HIAA has been found to promote insulin signaling in the context of TNF-α-induced hepatic IR, we speculated that the promotion of insulin signaling by 5-HIAA might rely on its

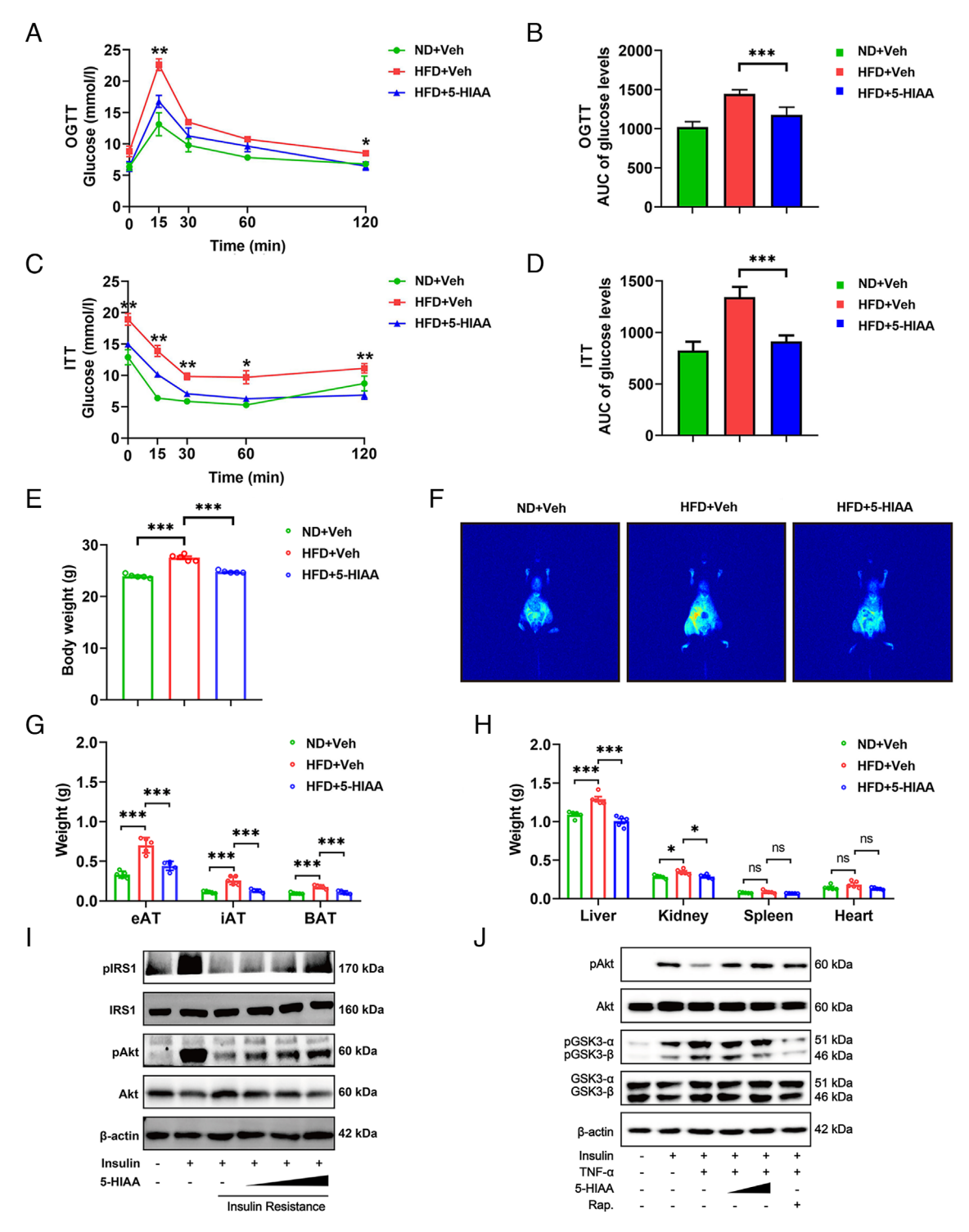


Fig. 4. Microbiota-dependent 5-HIAA improves glucose intolerance and obesity in HFD-fed mice, while preserving hepatic insulin sensitivity. (A-D) Effects of 5-HIAA on glucose intolerance in vivo. Male C57BL/6J mice (6 wk old; n = 5 per group) were fed a HFD or ND for 6 wk, with oral administration of 5-HIAA or vehicle (Veh) twice a day. After a 12 h (OGTT)/3 h (ITT) fasting at the end point, glucose levels and glucose area under the curve (AUC) were determined using the oral glucose tolerance test (OGTT) (A and B) and insulin tolerance test (ITT) (C and D). (E) Effects of 5-HIAA on body weights in vivo. (F) Effects of 5-HIAA on the distribution of fat mass and lean mass in vivo. (G) Effects of 5-HIAA on adipose tissue weights in vivo. (H) Effects of 5-HIAA on organ weights in vivo. (l) Effect of 5-HIAA on the insulin-stimulated IR in mice primary hepatocytes. Mice primary hepatocytes were treated with an increasing dosage of 5-HIAA (0.5, 1.5, and 4 mM) in the presence of high-concentration insulin (789 mM) for 24 h to induce IR, followed by insulin (5 nM) stimulation for 10 min after PBS washing. The protein levels of phosphorylated IRS1 at tyrosine 621 (pIRS1), IRS1, phosphorylated Akt (pAkt), and Akt were examined by immunoblotting. β-actin was used as a loading control. (/) HepG2 cells were treated with 5-HIAA (2 and 4 mM) and rapamycin (Rap.) for 24 h in the presence of TNF-α (200 ng/mL), followed by insulin (5 nM) stimulation for 10 min after PBS washing. The protein levels of pAkt, Akt, phosphorylated GSK-3 (pGSK-3), and GSK-3 were examined by immunoblotting. Each symbol represents an individual mouse (A-H). Data are shown as mean \pm SEM. (n=5) or are representative of three independent experiments with similar results (I and I). *P < 0.05, **P < 0.01, and ***P < 0.005; ns, not significant. Statistical analysis was performed using the Bonferroni post hoc test followed by one-way ANOVA (B, D, E, G, and H) or Tukey's post hoc test followed by one-way ANOVA (A and C).

function to inhibit the activation of mTORC1 signaling. To test this hypothesis, TNF- α -induced IR HepG2 cells were treated with 5-HIAA and the well-known mTORC1 inhibitor Rapamycin (Rap.). The phosphorylation of S6K1, as a result of mTORC1 activation, was obviously elevated by TNF- α stimulation in HepG2 cells (Fig. 5A). Treatment with both Rap. and 5-HIAA suppressed the mTORC1-mediated phosphorylation of S6K1, indicating that 5-HIAA inhibits the activation of mTORC1 signaling.

It is well established that tuberous sclerosis complex 2 (TSC2) acts as an upstream negative regulator of mTORC1 and is involved in the insulin signaling (24-26). We thus hypothesized that 5-HIAA functions at TSC2 to inhibit mTORC1 signaling. As expected, treatment of HepG2 cells with 5-HIAA dose dependently stimulated TSC2 gene transcription and thus increased its protein levels (Fig. 5 B and C). To further address whether TSC2 is required for the inhibition of the mTORC1 pathway by 5-HIAA, we examined the impacts of 5-HIAA on mTORC1 activation in the context of TSC2 knockdown. Pairs of siRNA targeting TSC2 gene (si-TSC2) were introduced into HepG2 cells and tested for the knockdown efficiency (Fig. 5D). When TSC2 expression was masked by the siRNA-mediated knockdown, 5-HIAA treatment could not suppress the provoked S6K1 phosphorylation resulted from the TNF-α-stimulated mTORC1 activation any more, suggesting that TSC2 directly involves the 5-HIAA-mediated inhibition of mTORC1 pathway (Fig. 5*E*). These data together imply that 5-HIAA inhibits the TSC2-mTORC1 pathway, thereby promoting hepatic insulin signaling in the context of IR.

We next sought to dissect the mechanism by which 5-HIAA stimulates TSC2 gene expression. AhR is a ligand-activated pleiotropic receptor that acts both as a transcription factor and as an E3 ubiquitin ligase, thus playing dual roles in regulating the levels of intracellular proteins (27). Previous studies demonstrated that TSC2 undergoes the methylation-mediated transcriptional repression by H3K9 histone methyltransferase (H3K9m3)/Suv39h1, while activated AhR can promote the ubiquitin-proteasome degradation of Suv39h1 via its function as an E3 ligase (27). Since 5-HIAA was recently suggested to activate the AhR signaling in regulatory B cells (28), we sought to examine whether 5-HIAA acts as a ligand to activate hepatic AhR and the downstream signaling. The docking model showed an interaction of 5-HIAA with the AhR-LDB domain responsible for the ligand binding (29), indicating that 5-HIAA can activate AhR in a ligand-dependent manner (SI Appendix, Fig. S9). This conception was further supported by the data from cellular experiments, as both 5-HIAA and the commercial AhR agonist FICZ markedly up-regulated the mRNA and protein levels of CYP1A1, an early biomarker of AhR activation (Fig. 5 F and G). Meanwhile, degradation of Suv39h1 in HepG2 cells was detected under the treatment with 5-HIAA and FICZ, indicating a direct activation of AhR by 5-HIAA (Fig. 5*G*).

To verify the essential role of AhR in the inhibition of mTORC1 pathway and promotion of insulin signaling by 5-HIAA, we determined the impacts of AhR knockdown on the functions of 5-HIAA. Under the scrambled siRNA (si-Control) treatment, 5-HIAA suppressed the phosphorylation of mTORC1 substrate S6K1 in TNF-α-stimulated HepG2 cells; while this activity of 5-HIAA was abolished in the context of AhR knockdown by si-AhR-1 treatment (Fig. 5 *H* and *I*). In addition, si-AhR-1 treatment reversed the 5-HIAA-promoted phosphorylation of Akt (Fig. 5 *J*). These results establish an upstream role of AhR in TSC2-mTORC1 signaling, which is inhibited by 5-HIAA to promote hepatic insulin signaling. To demonstrate the in vivo role of AhR in 5-HIAA-mediated improvement of glucose intolerance,

we investigated the diet-dependent influences of 5-HIAA on blood glucose levels and insulin sensitivity in AhR knockout (AhR-KO) mice and WT mice. 5-HIAA reduced glucose tolerance in the HFD-fed WT mice but had no effects in the HFD-fed AhR KO mice (Fig. 5 K and L). Our studies provide in vitro and in vivo evidence that 5-HIAA inhibits the TSC2-mTORC1 pathway through AhR.

T2D Patients Exhibit Decreased Levels of 5-HIAA. To explore the physiological significance of 5-HIAA in T2D development, we examined whether T2D patients undergo alterations of 5-HIAA levels. Subjects with and without T2D were recruited and targetedly measured the serum and urine levels of 5-HIAA (SI Appendix, Table S1). Individual fecal fermentation was also conducted to determine the capabilities of microbiota in producing 5-HIAA. Consistent with our initial observation that 5-HIAA concentrations were lower in HFD-induced IR mice than ND-fed mice, decreased 5-HIAA levels were found in fermentation broth of fecal bacteria from subjects with T2D (T2D; n = 21) versus without T2D (no T2D, H; n = 15) (Fig. 6A). Meanwhile, the serum levels of 5-HIAA were diminished in T2D patients (T2D; n = 23) compared to healthy subjects (no T2D; n = 22) (Fig. 6B). It was noticed that the urine concentrations of 5-HIAA were nearly 10-fold relative to serum levels, supporting the notion that the circulating 5-HIAA originated from the gut is mainly excreted in the urine (30). Although the urine levels of 5-HIAA showed no significant difference (P = 0.059) between two groups, we still observed a downtrend in subjects with T2D (Fig. 6C). These findings suggest that the decreased circulating 5-HIAA levels is a hallmark of T2D.

Discussion

Numerous studies have shown that the gut microbiota composition is altered in a HFD regimen, suggesting that this gut dysbiosis could drive various phenotypic changes and progression of HFDassociated diseases such as T2D (31). In this study, we dissected the HFD-induced alterations in the gut microbiome and metabolome of mice with IR, and displayed certain metabolism pathways that were impaired under the gut dysbiosis. As previously observed in the gut microbiomic profile of people with obesity (18), the *Bacteroidetes* to *Firmicutes* ratio was decreased in the gut microbial composition of HFD mice. On the other side, the Trp metabolic pathway came out on Top 5 in the list of impaired metabolism pathways under HFD. The integrated gut microbiomics and metabolomics data imply a tight connection among HFD-associated T2D, the gut microbiota, and intestinal Trp metabolism. Through the irregulated Trp metabolic pathway, a microbiota-dependent Trp metabolite 5-HIAA was found to be barely produced in HFD-induced IR mice as well as in T2D patients, and was further demonstrated to be capable of protecting hepatic insulin sensitivity, improving glucose intolerance, and reducing obesity in vivo. Therefore, our integrated gut microbiomic and metabolomic dataset might serve as a powerful tool to study the HFD-gut microbiota-host metabolism cross talk regarding T2D. To deeply analyze this dataset, exploring the correlations between T2D and other metabolic pathways is ongoing.

Host and microbiota cooperatively mediate intestinal Trp metabolism through the canonical 5-HT pathway. This pathway mainly occurs in ECs in the gut, where the host enzyme TPH1 transforms intestinal Trp into 5-HTP that is further catalyzed into 5-HT by AAAD. It is believed that the microbiota participate in the production of 5-HT, as some microbiota-derived metabolites (e.g., SCFAs and deoxycholate) have been demonstrated to

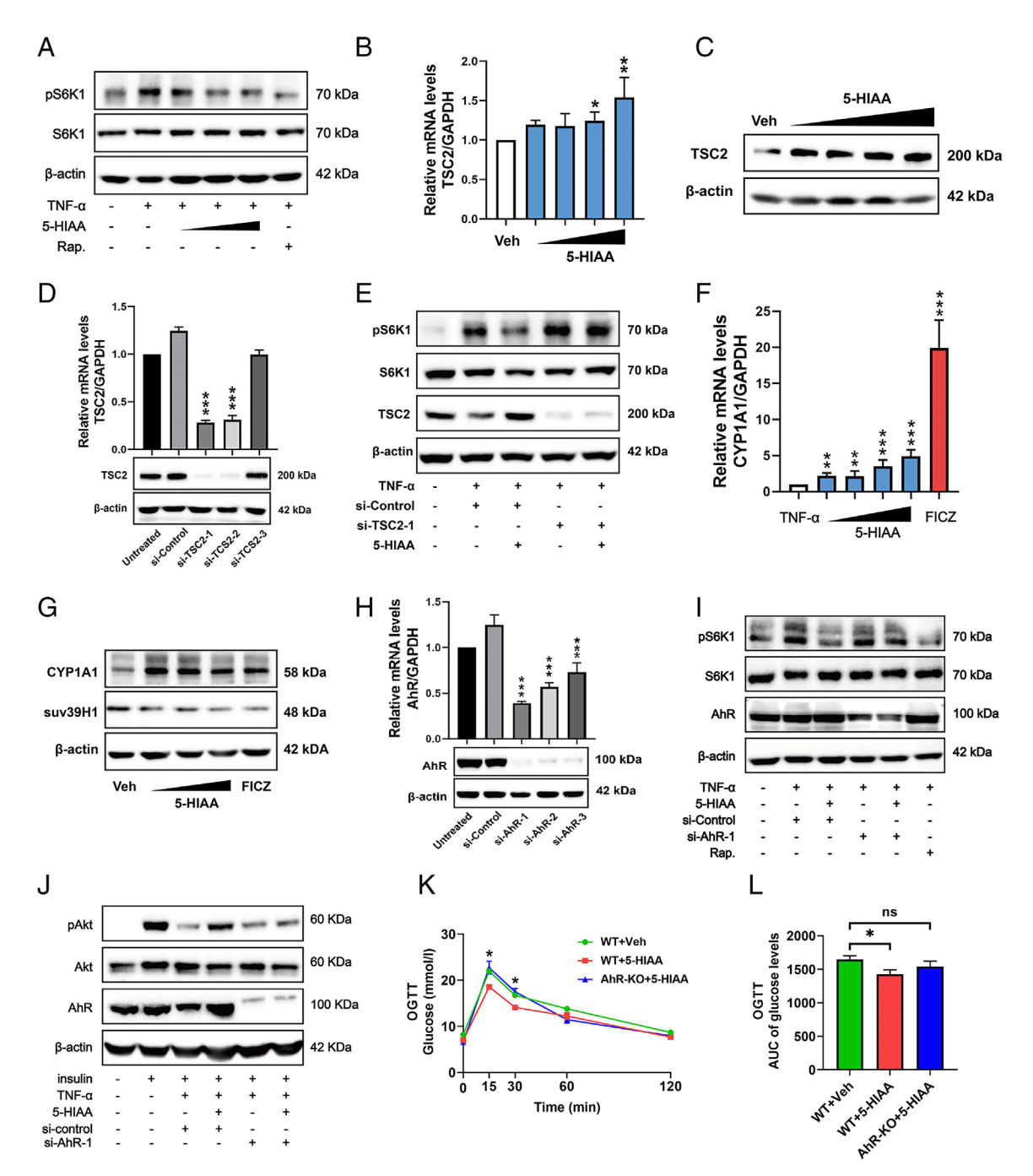


Fig. 5. 5-HIAA inhibits the TSC2-mTORC1 pathway via direct activation of AhR. (A) Inhibition of the mTORC1-mediated phosphorylation of S6K1 by 5-HIAA. HepG2 cells were mock-stimulated or stimulated with TNF- α (200 ng/mL) as described in Fig. 3 and were then treated with vehicle, the mTÓRC1 inhibitor rapamycin (Rap.) or a growing concentration of 5-HIAA (1, 2, and 4 mM) for 24 h. Cell lysates were subjected to immunoblotting for examining the protein levels of phosphorylated S6K1 at Thr389 (pS6K1) and S6K1. β-actin was used as a loading control. (B and C) Upregulation of TSC2 expression by 5-HIAA. HepG2 cells were treated with vehicle or an increasing dosage of 5HIAA (1, 2, 4, and 8 mM) for 24 h. The relative mRNA levels (shown fold change) of TSC2 were determined by qPCR, and GAPDH mRNA was used as an internal control (B). The protein levels of TSC2 were examined by immunoblotting (C). (D) siRNA-mediated knockdown of TSC2 expression. HepG2 cells were mocktreated or treated with scrambled siRNA (si-Control) and pairs of siRNA specifically targeting *Tsc2* (si-TSC2-1/-2/-3). The protein and mRNA levels of TSC2 were examined by immunoblotting and qPCR, respectively. (*E*) Impacts of TSC2 knockdown on the inhibition of S6K1 phosphorylation by 5-HIAA. HepG2 cells were transfected with si-Control or si-TSC2 and were then treated with vehicle or 5-HIAA (4 mM) for 24 h in the presence of TNF-α (200 ng/mL). The protein levels of pS6K1, S6K1, and TSC2 were examined by immunoblotting. (F) Induction of the AhR activation biomarker CYP1A1 by 5-HIAA. HepG2 cells were treated with vehicle, the AhR ligand FICZ, or an increasing dosage of 5-HIAA (1, 2, 4, and 8 mM) for 24 h. The relative mRNA levels (shown as fold change) of CYP1A1 were determined by qPCR, and GAPDH mRNA was used as an internal control. (G) Promotion of Suv39h1/H3K9m3 degradation by 5-HIAA. Similar to (F), except that HepG2 cells were first stimulated with TNF-α (200 ng/mL) before the following treatment. The protein levels of CYP1A1 and Suv39h1 were examined by immunoblotting. β-actin was used as a loading control. (H) siRNA-mediated knockdown of AhR expression. HepG2 cells were mock-treated or treated with scrambled siRNA (si-Control) and pairs of siRNA specifically targeting the AhR gene (si-AhR-1/-2/-3). The protein and mRNA levels of AhR were examined by immunoblotting and qPCR, respectively. (/) Impacts of AhR knockdown on the inhibition of S6K1 phosphorylation by 5-HIAA. HepG2 cells were transfected with si-Control or si-AhR-1 and were then treated with vehicle or 5-HIAA (4 mM) for 24 h in the presence of TNF-α (200 ng/mL). Treatment with the mTORC1 inhibitor Rapamycin (Rap.) was a positive control. The protein levels of pS6K1, S6K1, and AhR were examined by immunoblotting. (/) Impacts of AhR knockdown on the upregulation of Akt phosphorylation by 5-HIAA. Similar to (/), except that HepG2 cells were prestimulated with insulin (5 nM). The protein levels of pAkt, Akt, and AhR were examined by immunoblotting. (K and L) Impacts of AhR deficiency on the bioactivity of 5-HIAA in improving glucose intolerance in vivo. Male wild-type (WT) and AhR-KO C57BL/6J mice (6 wk old; n = 5 per group) were treated as described in Fig. 3. Glucose levels and glucose AUC were determined using OGTT. Data are from three independent experiments (B, D, F, and B, mean B SD.) or five (B and B, mean B SD.) biological replicates or are representative of three independent experiments with similar results (B, B, B, B, B, B, B). The independent experiments with similar results (B, B, B, B) and B, B0. Statistical analysis was performed using unpaired two-tailed Student's t test (B, D, F, and H), Bonferroni post hoc test followed by one-way ANOVA (L), or Tukey's post hoc test followed by one-way ANOVA (K).

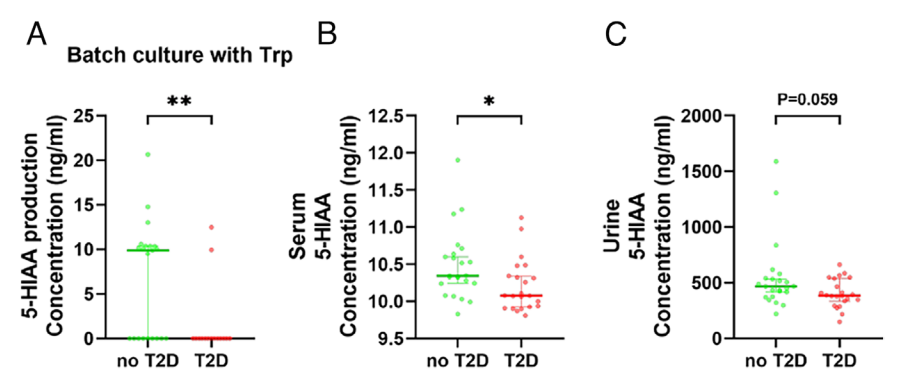


Fig. 6. Levels of 5-HIAA are diminished in subjects with type 2 diabetes. (A) Fecal bacteria suspensions were obtained from subjects without type 2 diabetes (no T2D, n = 21) and with T2D (T2D, n = 15) and were then incubated with Trp (10 mM) for 24 h. The concentration of 5-HIAA was measured by targeted HPLC-MS/MS analysis. (B and C) Serum and urine were collected from subjects without T2D (no T2D, n = 23) and with T2D (T2D, n = 22). Targeted HPLC-MS/MS analysis was conducted to determine the intensity of 5-HIAA in each sample. Each symbol represents an individual subject. Data are shown as median \pm 95% CI. *P < 0.05 and **P < 0.01. Statistical analysis was performed using the Mann-Whitney test.

stimulate the 5-HT biosynthesis (11, 12). Besides its regulatory role in intestinal Trp metabolism, gut microbiota has been demonstrated herein to be capable of transforming Trp into 5-HIAA. Our data suggest that the microbial catalysis pathway for producing 5-HIAA from Trp is independent of the canonical 5-HT pathway and is most probably mediated by *Burkholderia* spp. We thus speculate that the gut microbiota play a dual role in intestinal Trp metabolism: both as a regulator of the host-dependent 5-HT pathway and as a director of a noncanonical microbiota-dependent pathway. Future studies are ongoing to identify the specific 5-HIAA-producing bacteria and determine the role of the gut microbiota in intestinal Trp metabolism.

AhR, a nuclear receptor equipped in various cell types, has emerged as an environmental sensor to detect both xenobiotics and endogenous ligands derived from diet, the microbiota, and the host (16). Recently, Trp-derived metabolites are considered as an important family among the microbiota-dependent physiological ligands of AhR. For instance, the Trp metabolites tryptamine and indole-3-acetic acid can directly bind to AhR (32, 33). In addition, kynurenic acid was reported to activate AhR in immune cells (34), while restoring AhR signaling exert beneficial effects on metabolic syndrome (35). As aforementioned, certain microbiota can process Trp into indoles and its three-substituted derivatives which act as AhR agonists (36). In this study, we did not detect obvious variation in the levels of Trp or its metabolites (e.g., tryptamine and Kyn) known to activate AhR between ND mice and HFD mice. Yet we observed a reduction in 5-HIAA under the HFD-induced gut dysbiosis and further uncovered that 5-HIAA acts as an AhR ligand to activate the downstream signaling in hepatic cells. As illustrated in our proposed model (7), circulating 5-HIAA derived from intestinal Trp enters hepatic cells and activates AhR in a ligand-dependent manner. The activated AhR promotes the ubiquitin-proteasome degradation of Suv39h1 via its E3 ligase activity, thereby stimulating TSC2 expression which could inhibit the activation of mTORC1 signaling. Since the HFD-induced hyperactivation of mTORC1 reduces the tyrosine phosphorylation of IRS1 and suppresses the subsequent activation of Akt, the action of 5-HIAA through the AhR/TSC2/mTORC1 axis would promote hepatic insulin signaling, improve glucose intolerance, and reduce obesity. Once the microbial production of 5-HIAA is suspended owing to the HFD-induced gut dysbiosis, the hepatic insulin signaling and glucose homeostasis would be irregulated. Our findings thus partially explore the issues and underlying mechanisms of the HFD-microbiota-Trp metabolism interplay regarding T2D.

Our study uncovered that 5-HIAA can effectively alleviate the HFD-induced glucose intolerance and obesity in vivo. This finding highlights the potential of 5-HIAA as a therapeutic agent for the metabolic syndromes characterized by IR and glucose intolerance. Considering that colonization of engineered gut bacteria stimulating the production of 5-HIAA in the gut might be a promising therapy for these metabolic disorders. More importantly, we have proved that the microbiota-dependent 5-HIAA is also associated with T2D, as the T2D subjects show decreased 5-HIAA concentrations in sera. Whether 5-HIAA can be employed as a biomarker for T2D diagnosis requires a larger cohort study. Our present work implies a negative correlation between 5-HIAA levels and T2D development.

Materials and Methods

Ethics and Human Subjects. All surgical procedures were approved by the Institutional Animal Care and Use Committee (IACUC) of Zhejiang University of Technology. All work was approved by the Medical Ethical Committee of the Ningbo First Hospital (Ningbo, Zhejiang, China). Informed consent was obtained from all participants, and all participants were evaluated and treated by licensed medical professionals at Ningbo First Hospital in Ningbo, Zhejiang, China.

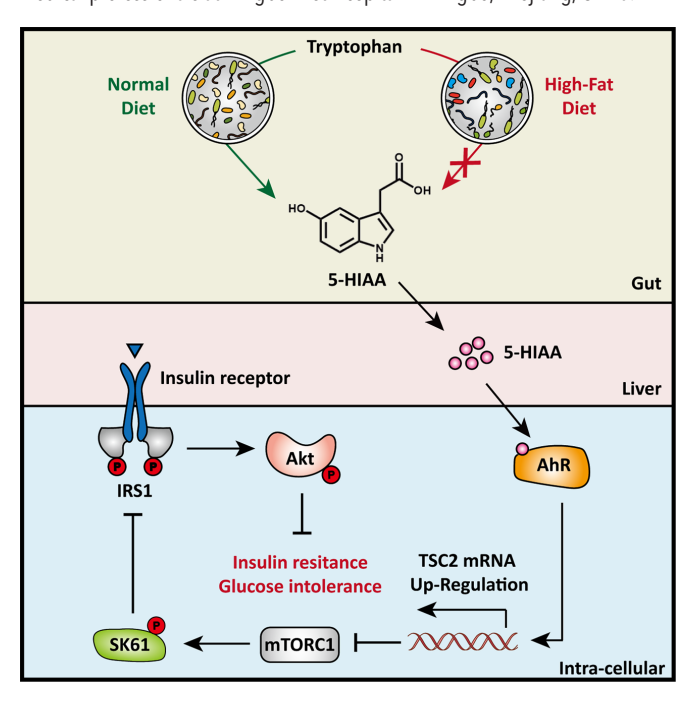


Fig. 7. A model for the promotion of hepatic insulin signaling by 5-HIAA through the AhR/TSC2/mTORC1 axis.

Quantification and Statistical Analysis. Metastats software for metagenomics sequencing data was utilized to characterize the microbial communities. CD-HT and R statistical software were used for BIOM-formatted OTU communities clustering and OTU statistics. The difference in the alpha diversity between ND and HFD mice was tested using the Mann-Whitney U test (SPSS 20.0), and P-values were adjusted with FDR (below 5%). Alpha diversity was applied to analyze the complexity of species diversity for a sample through four indices, including Chao1, Shannon, Simpson, and Observed species. All these indices in our samples were calculated with QIIME (version 1.8.0). Beta diversity analysis was used to evaluate differences in samples in species complexity. Beta diversity was calculated by PCA and cluster analysis by QIIME software (version 1.8.0). For untargeted metabolomics, the fold-change analysis and t test were used to obtain q-values by BH correction and VIP (Variable Important for the Projection) values (The screening condition was set as $VIP \ge 1.0$.) obtained by PLS-DA, which were utilized to screen differentially expressed metabolic ions between ND and HFD mice. Otherwise, Bonferroni post hoc test followed by one-way ANOVA, Tukey's post hoc test followed by one-way ANOVEA, and unpaired two-tailed Student's t tests were used, as indicated.

Data, Materials, and Software Availability. All the materials and methods conducted in this study are detailed in SI Appendix, Materials and Methods: mice and diet, cell lines, liver resection and pulverization, 16S rDNA sequencing, analysis of sequencing data, species annotation and abundance

- C. Aurelie et al., Dietary intervention impact on gut microbial gene richness. Nature 500, 585-588
- E.-L. Chatelier et al., Richness of human gut microbiome correlates with metabolic markers. Nature 500, 541-546 (2013).
- J. Qin et al., A metagenome-wide association study of gut microbiota in type 2 diabetes. Nature 490, 55-60 (2012).
- H.-M. Roager, T.-R. Licht, Microbial tryptophan catabolites in health and disease. Nat. Commun. 9,
- M.-S. Brown, J.-L. Goldstein, Selective versus total insulin resistance: A pathogenic paradox. Cell Metab. 7, 95-96 (2008).
- M. Ruiz-Canela et al., Plasma branched chain/aromatic amino acids, enriched Mediterranean diet and risk of type 2 diabetes: Case-cohort study within the PREDIMED Trial. Diabetologia 61, 1560-1571 (2018)
- D. Preiss et al., Effect of metformin therapy on circulating amino acids in a randomized trial: The CAMERA study. Diabetic Med. 33, 1569–1574 (2016).
- D. Dodd et al., A gut bacterial pathway metabolizes aromatic amino acids into nine circulating metabolites. Nature 3, e00438 (2017).
- A. Agus, J. Planchais, H. Sokol, Gut microbiota regulation of tryptophan metabolism in health and disease. Cell Host Microbe 23, 716-724 (2018).
- P.-J. Kennedy, J.-F. Cryan, T.-G. Dinan, G. Clarke, Kynurenine pathway metabolism and the microbiota-gut-brain axis. Neuropharmacology 112, 399-412 (2017).
- C.-S. Reigstad et al., Gut microbes promote colonic serotonin production through an effect of short-chain fatty acids on enterochromaffin cells. FASEB J. 29, 1395-1403 (2015)
- J. Yano et al., Indigenous bacteria from the gut microbiota regulate host serotonin biosynthesis. Cell. 161, 264-276 (2015).
- 13. R.-L. Young et al., Augmented capacity for peripheral serotonin release in human obesity. Int. J. Obes. (Lond). 42, 1880-1889 (2018).
- G. Sumara, O. Sumara, J.-K. Kim, G. Karsenty, Gut-derived serotonin is a multifunctional determinant to fasting adaptation. Cell Metab. 16, 588-600 (2012).
- 15. A.-M. Martin et al., The gut microbiome regulates host glucose homeostasis via peripheral serotonin. Proc. Natl. Acad. Sci. U.S.A. 116, 19802-19804 (2019).
- L. Zhou, AHR function in lymphocytes: Emerging concepts. *Trends Immunol.* 37, 17–31 (2016).
- I. Monteleone, F. Pallone, G. Monteleone, Aryl hydrocarbon receptor and colitis. Semin. 17 Immunopathol. 35, 671-675 (2013).
- R.-E. Ley, P.-J. Turnbaugh, S. Klein, J.-I. Gordon, Microbial ecology: Human gut microbes associated
- with obesity. Nature. 444, 1022-1023 (2006). S. Hodge, B.-P. Bunting, E. Carr, J.-J. Strain, B.-J. Stewart-Knox, Obesity, whole blood serotonin and
- sex differences in healthy volunteers. Obes. Facts 5, 399-407 (2012). X. Shi et al., Hydroxytryptophan biosynthesis by a family of heme-dependent enzymes in bacteria. Nat. Chem. Biol. 19, 1415-1422 (2023).

analysis of metagenomic sequencing, metabolite extraction, untargeted metabolomic profiling, antibiotic treatment, sequence alignment, glucose tolerance test (OGTT) and insulin tolerance test (ITT), immunoblotting, liquid chromatography-mass spectrometry (LC-MS), apparent enzyme kinetics assay, heterologous overexpression of TMO and laaH in E. coli DH5 α , in vitro fermentations, and molecular docking. All other data are included in the manuscript and/or SI Appendix. The 16S rDNA gene sequences have been deposited in the National Center for Biotechnology Information database (NCBI Accession: PRJNA1102001) (37).

ACKNOWLEDGMENTS. This work was supported by grants from the National Natural Science Foundation of China (22134003) and National Key Research and Development Program of China (2018YFA0900404). We thank Dr. Yanjing Li (East China University of Science and Technology) for the insightful discussion.

Author affiliations: aLab of Biosystems and Microanalysis, State Key Laboratory of Bioreactor Engineering, East China University of Science and Technology, Shanghai 200237, China; bInstitute of Engineering Biology and Health, Collaborative Innovation Center of Yangtze River Delta Region Green Pharmaceuticals, College of Pharmaceutical Sciences, Zhejiang University of Technology, Hangzhou 310014, Zhejiang, China; ^cDepartment of Endocrinology and Metabolism, Ningbo First Hospital, Ningbo 315010, Zhejiang, China; and ^dGuangzhou National Laboratory, Guangzhou International Bio-Island, Guangzhou 510005, Guangdong, China

- 21. Y. Liu, Y. Hou, G. Wang, X. Zheng, H. Hao, Gut microbial metabolites of aromatic amino acids as signals in host-microbe interplay. Trends Endocrinol. Metab. 31, 818-834 (2020).
- W.-H. Tang et al., Intestinal microbial metabolism of phosphatidylcholine and cardiovascular risk. N. Engl. J. Med. 368, 1575-1584 (2013).
- 23. O.-N. Ozes et al., A phosphatidylinositol 3-kinase/Akt/mTOR pathway mediates and PTEN antagonizes tumor necrosis factor inhibition of insulin signaling through insulin receptor substrate-1. Proc. Natl. Acad. Sci. U.S.A. 98, 4640-4645 (2001)
- 24. Y. Li, M.-N. Corradetti, K. Inoki, K.-L. Guan, TSC2: Filling the GAP in the mTOR signaling pathway. Trends Biochem. Sci. 29, 32-38 (2004).
- E.-V. Haar, S.-I. Lee, S. Bandhakavi, T.-J. Griffin, D.-H. Kim, Insulin signalling to mTOR mediated by the Akt/PKB substrate PRAS40. Nat. Cell Biol. 9, 316–323 (2007).
- Y. Cao et al., Interaction of FoxO1 and TSC2 induces insulin resistance through activation of the mammalian target of rapamycin/p70 S6K pathway. J. Biol. Chem. 281, 40242-40251 (2006).
- 27. Y. Miao et al., Alpinetin improves intestinal barrier homeostasis via regulating AhR/suv39h1/TSC2/ mTORC1/autophagy pathway. Toxicol. Appl. Pharmacol. 384, 114772 (2019)
- E.-C. Rosser et al., Microbiota-derived metabolites suppress arthritis by amplifying aryl hydrocarbon receptor activation in regulatory B cells. Cell Metab. 31, 837-851.e810 (2020).
- W.-H. Bisson et al., Modeling of the aryl hydrocarbon receptor (AhR) ligand binding domain and its utility in virtual ligand screening to predict new AhR ligands. J. Med. Chem. 52, 5635-5641
- J.-B. Corcuff, L. Chardon, I.-E. Ridah, J. Brossaud, Urinary sampling for 5HIAA and metanephrines determination: Revisiting the recommendations. Endocr. Connect. 6, R87-R98 (2017).
- 31. A. Koh et al., Microbially produced imidazole propionate impairs insulin signaling through mTORC1. Cell. 175, 947-961.e17 (2018).
- S. Heath-Pagliuso et al., Activation of the Ah receptor by tryptophan and tryptophan metabolites. Biochemistry 37, 11508-11515 (1998).
- L.-V. Bergander, W. Cai, B. Klocke, M. Seifert, I. Pongratz, Tryptamine serves as a proligand of the AhR transcriptional pathway whose activation is dependent of monoamine oxidases. Mol. Endocrinol. 26, 1542-1551 (2012).
- S.-H. Seok et al., Trace derivatives of kynurenine potently activate the aryl hydrocarbon receptor (AHR). J. Biol. Chem. 293, 1994-2005 (2018).
- J.-M. Natividad et al., Impaired aryl hydrocarbon receptor ligand production by the gut microbiota is a key factor in metabolic syndrome. Cell Metab. 28, 737-749.e734 (2018).
- M.-K. Rasmussen, P. Balaguer, B. Ekstrand, M. Daujat-Chavanieu, S. Gerbal-Chaloin, Skatole (3-Methylindole) is a partial aryl hydrocarbon receptor agonist and induces CYP1A1/2 and CYP1B1 expression in primary human hepatocytes. PLoS ONE 11, e0154629 (2016).
- W. Du, Data from "Comparison of the microbiome of fecal samples from mice on a normal diet and mice on a high-fat diet." NCBI. https://www.ncbi.nlm.nih.gov/bioproject/PRJNA1102001/. Accessed 18 April 2024.